JOURNAL OF MATERIALS SCIENCE **37** (2002) 3107–3116

Fabrication of soft tissue engineering scaffolds by means of rapid prototyping techniques

R. LANDERS, A. PFISTER
Freiburger Materialforschungszentrum and Institut für Makromolekulare Chemie der Albert-Ludwigs-Universität Freiburg, D-79104 Freiburg, Germany
E-mail: landers@fmf.uni-freiburg.de

U. HÜBNER
Klinik für Mund-Kiefer und Gesichtschirurgie, Klinikum der Albert-Ludwigs-Universität Freiburg, D-79095 Freiburg, Germany

H. JOHN
Envision Technologies GmbH, Elbestr. 10, D-45768 Marl, Germany
E-mail: www.envisiontec.de

R. SCHMELZEISEN
Klinik für Mund-Kiefer und Gesichtschirurgie, Klinikum der Albert-Ludwigs-Universität Freiburg, D-79095 Freiburg, Germany

R. MÜLHAUPT*
Freiburger Materialforschungszentrum and Institut für Makromolekulare Chemie der Albert-Ludwigs-Universität Freiburg, D-79104 Freiburg, Germany
E-mail: mulhaupt@fmf.uni-freiburg.de

Scaffolds are of great importance for tissue engineering because they enable the production of functional living implants out of cells obtained from cell culture. These scaffolds require individual external shape and well defined internal structure with interconnected porosity. The problem of the fabrication of prototypes from computer assisted design (CAD) data is well known in automotive industry. Rapid prototyping (RP) techniques are able to produce such parts. Some RP techniques exist for hard tissue implants. Soft tissue scaffolds need a hydrogel material. No biofunctional and cell compatible processing for hydrogels exists in the area of RP. Therefore, a new rapid prototyping (RP) technology was developed at the Freiburg Materials Research Center to meet the demands for desktop fabrication of hydrogels. A key feature of this RP technology is the three-dimensional dispensing of liquids and pastes in liquid media. The porosity of the scaffold is calculated and an example of the data conversion from a volume model to the plotting path control is demonstrated. The versatile applications of the new hydrogel scaffolds are discussed, including especially its potential for tissue engineering.

1. Introduction

Tissue engineering is a rapid developing new area of science and many exciting results have been published recently [1]. The main focus of tissue engineering was on the culture of cells for the last ten years. The generation of functional implants from living cells becomes now more and more important. Therefore, the three dimensional (3D) structure and its generation begins to play an essential role. In general, organs are 3D structures composed out of living cells and a support structure. According to their mechanical strengths the supports can be classified as soft and hard tissue.

For the generation of 3D implants out of a cell culture special biodegradable and biocompatible scaffolds are required. They should be replaced by the natural support structure after degradation and therefore considered only as a temporary support for cell growth and cell adhesion. The scaffold structure needs interconnecting pores to allow the 3D flow of culture medium or blood in order to ensure continuous supply of nutrients and metabolites which is of great importance for the survival of the cells cultured on the scaffold. The pores are considered to be in the range of 5–10 times of the cell diameter, typically 100–300 μm. Porous scaffolds facilitate tissue formation and provide an adequate mechanical strength required in future during transplantation and implantation in the human body. Furthermore, not only the internal structure of the scaffolds has to be

*Author to whom all correspondence should be addressed.

TABLE I Comparison of different RP technologies

RP technique	Materials	Advantage	Disadvantage
(CNC milling)	Ceramics, bulk polymers	Broad range of bulk materials Excellent mechanical strength	No complex internal structure
Laser sintering	Metals, ceramics, bulk polymers, compounds	High accuracy Good mechanical strength Broad range of bulk materials	Elevated temperatures—local high energy input Uncontrolled porosity
Stereolithography	Reactive resins	Good mechanical strength	Limited to reactive resins (mostly toxic)
Inkjet printing	Wax or wax compounds	Excellent accuracy	Slow process Material limited to low melting point wax
3D printing (MIT)	Ink + powder of bulk polymers, ceramics	No inherent toxic components Fast processing Low costs	Weak bonding between powder particles Bad accuracy—rough surface
FDM/FDC	Some thermoplastic polymers/ceramics	Low costs	Elevated temperatures Small range of bulk materials Medium accuracy
3D plotting	Swollen polymers (hydrogels), thermoplastic polymers, reactive resins, ceramics	Broad range of materials Broad range of conditions Incorporation of cells, proteins and fillers	Slow processing Low accuracy No standard condition—time consuming adjustment to new materials

tailored according to the different implant applications but also the external shape needs to fit the individual requirements of each patient. The problem of producing individual parts with complex internal as well as external structures is a key feature of rapid prototyping (RP) technologies, used especially in the automotive industry [2]. An increasing number of techniques and machines are summarised by this technical term, but all of them are based on the layered manufacturing process. A computer model (volume model) is sliced into a number of layers by a CAD software and each layer of the original model is produced in succession. An overview of some important RP technologies and CNC milling including their advantages and disadvantages regarding their use in the biomedical field is given in Table I. Technical descriptions of the different RP techniques in general have been reviewed [2].

The general vision of combining modern medical 3D analytical tools, CAD, tissue engineering and rapid prototyping is shown in Fig. 1. The desired implant area of the patient is scanned by X-ray or magnetic resonance and the data are imported into a CAD software. This software enables the surgeon to design the implant according to the individual requirements. The information is transferred to a RP system, which produces the scaffold from a biocompatible and biodegradable material. Living cells are seeded onto the surface of the scaffold after production or integrated into the RP process. After a cell culture treatment and a cell number enlargement the implant is brought into the human body and starts to fulfil its function. The material disappears after a time and is replaced by natural tissue.

Many details of this vision are still reality like data acquisition, CAD, biomaterial design or cell culture of human cells, but internal organs are composed out of many different cell types at different places. Cell seeding after scaffold production onto the scaffold surface is well established but does not allow the segmentation of the scaffold regarding the cell type. It would be very interesting to incorporate living cells into the RP process. In this case the CAD software, in combination with the RP system, would define shape and the cell type at specific scaffold regions. Some attempts have been made in the past to combine the favourable RP technologies with the biomedical problem of generating individual scaffolds. For hard tissue implants the traditional CNC milling of titanium parts is known for some years. Although CNC milling is not a RP technology and is unable to produce complex internal structures the process is well established for artificial hips or skull plates and the process is totally computer controlled. Application of RP technology in the biomedical field, especially in drug release, was pioneered by Cima and coworkers who used bonding of powder by means of ink-jet printing of a binder which swells and bonds together individual powder particles via interdiffusion of polymer chains. In their process, which became known as 3D Printing^{TM}, poly(lactide) powder is bonded together layer-by-layer [3]. Since poly(lactide) is water insoluble, chloroform has been used as organic binder [4]. Stereolithography (STL) is limited to photopolymerization of frequently toxic resins which limit applications in scaffold fabrication. During selective laser sintering (SLS) the materials are exposed to high temperatures which are prohibitive to many biodegradable and biofunctional materials. Hutmacher and coworkers reported melt processing of thermoplastic biodegradable polymers such as polycaprolactone (PCL) by means of fused deposition modeling (FDM) [5]. Filaments of polymers are fed into a heated nozzle which melts the polymer and affords the 3D positioning of the polymer melts to form strands. Biodegradable scaffolds prepared by FDM are currently being evaluated as carriers for osteoblasts [6]. It appears likely that hard tissue replacement (bone) will be successful with FDM-based scaffolds. Possibilities and requirements of soft tissue implants are different. Soft tissue has a very high content of water. In fact it is build up by living cells and the extracellular matrix, which keeps the cells at the right place and determines the mechanical strength. From the chemical point of view it is a hydrogel, which means a water swollen polymer network. Although its chemistry and structure is tailored in detail by nature, also a standard hydrogel like alginic acid exhibits some

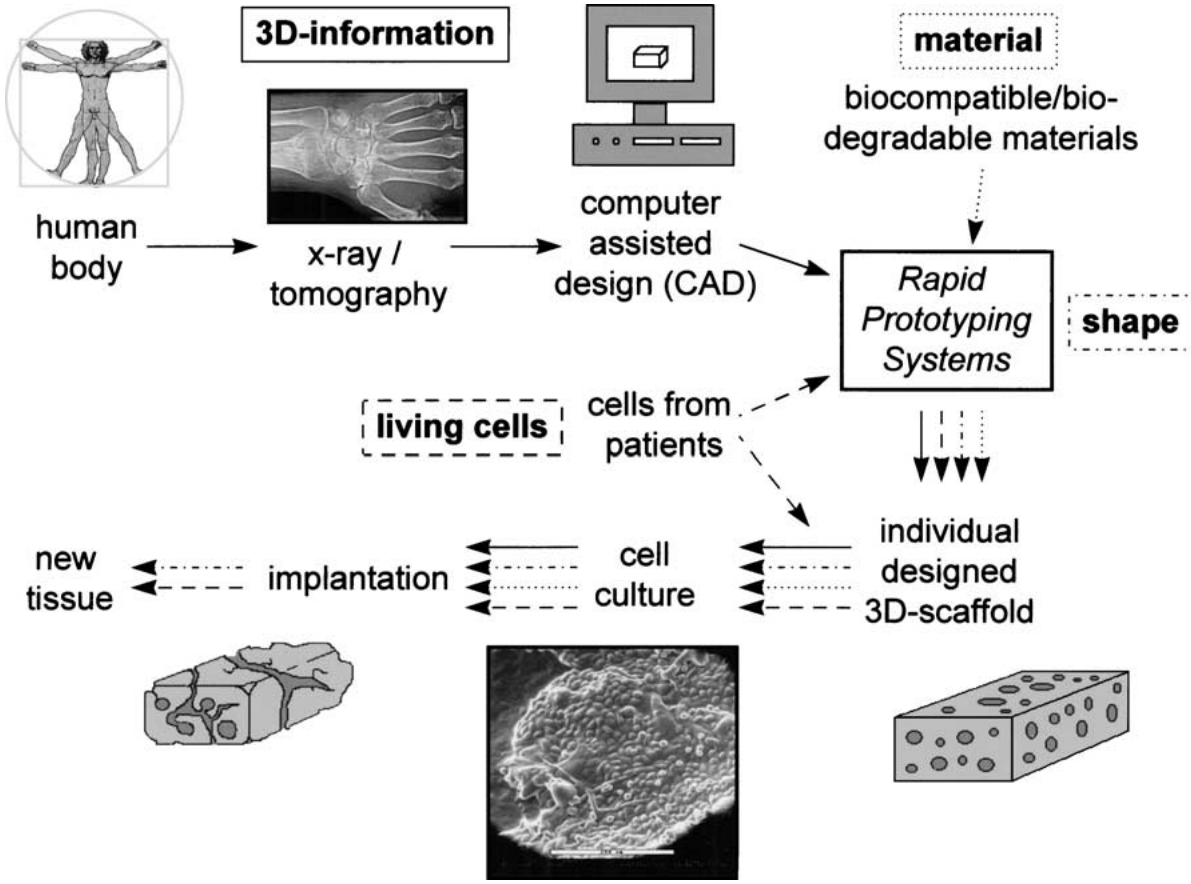

Figure 1 Vision of biomedical RP.

of the advantageous properties. A broad range of hydrogels from natural as well as synthetic sources is suitable for tissue engineering applications [7]. Hydrogels are flexible and allow the diffusion of hydrophilic substrates. It is possible to incorporate cells into hydrogels, because oxygen, salts, nutrients and metabolites are supplied to or removed from the incorporated cells [8]. The content of dry polymer is low and therefore the degradation products of the polymer are on a low level which causes a reduced immune response. Although these are attractive opportunities, the major emphasis of scaffold fabrication, supported by rapid prototyping technologies, was placed upon melt and powder processing of biodegradable thermoplastics in the absence of water. The adjustment of the general vision for biomedical RP to the details of soft tissue implants determines several requirements. First of all the material has to be a hydrogel. Toxic contaminations (organic solvents for example) have to be avoided. The temperature should not exceed 37°C because otherwise proteins undergo a denaturation. The incorporation of growth factors into the scaffold would be attractive for tissue engineering. Furthermore, the range of hydrogel materials should be as broad as possible, because of the different mechanical and chemical conditions occurring in soft tissue. High resolution is not necessary because of the hydrogel flexibility. The processing conditions of STL, SLS as well as CNC milling prevent the usage of hydrogels. Furthermore, hydrogels have not been processed by 3D-printing™ or FDM. The standard RP techniques, tailored for industrial applications, do not fulfil the requirements for soft tissue implants and a new RP technology for the generation of scaffolds working under cell compatible conditions would be desirable.

2. Materials and methods

3D plotters allow computer-assisted design with computer-guided 3D dispensing in a liquid medium. The prototype of the 3D plotter was based on a CNC-milling machine (Diadrive 2000 from Mutronic Feingerätebau GmbH, Rieden, Germany) for 3D positioning of a dispenser. The milling head was removed and replaced by a metal double jacket cartridge. The double jacket cartridge was equipped with a standard Luer-Lock-adaption for the dispensing nozzles at the bottom and a screw at the top with a socket for the compressed air hose connected by a PTFE seal. A thermostat filled with thermal oil was used to heat the cartridge. The automatic dosing valve (Globaco, D-63322 Rödermark, Germany) was connected to the compressed air and the 3D plotter. A standard PC controlled the CNC milling machine and the dosing valve. The CNC-software (EdiTasc, Trimeta Software, Tiefenbronn, Germany) was modified to enable automatic control of the dispenser valve. The plotting medium was filled into a glass crystallisation dish with a diameter of 15 cm and a height of 5 cm. The nozzles of the dispenser were exchanged according the viscosity of the plotting material (low viscosity needs smaller needle diameters), but in most cases a cyanoacrylate tip with PTFE inlay (Globaco) was used. Insulation of the nozzles with a sealing resin or heating of the nozzle by a resistance heater prevent blockages due to gelation.

The fabrication conditions of the agar scaffold are described elsewhere [9]. The alginate scaffolds were prepared by plotting of a 5% aqueous solution of sodium alginate with 1% gelatin and 0.1% ethylenediamine tetraacetic acid (EDTA) into a 0.03 mol/l aqueous solution of calcium chloride. The bottom of the plotting basin was covered by a rough cardboard. The air pressure reached values between 1.5×10^5 and 2.0×10^5 Pa and the temperature was around 25°C. The plotting head moved with a speed of 13 mm/s. The repeat lengths varied between 0.5 and 1.4 mm for the xy-direction and 0.3 and 0.35 mm for the vertical direction. The nozzle was a cyanacrylate tip (Globaco) with an inner diameter of 0.15 mm. But the strand diameter was in the range of 0.35 mm. The delay at 90° turning points was 0.06 s.

The fibrin/alginic acid scaffolds were prepared by plotting a mixture of alginic acid with fibrinogen into a solution of calcium chloride, thrombin and sodium chloride. Sodium chloride is required for adjustment of an isotonic osmotic pressure. 5 ml of the plotting material were produced by mixing 4.5 ml of a 7% alginic acid solution with 0.1% EDTA and 0.5 ml of a fibrinogen solution (prepared according to the instructions of the fibrin glue). 20 ml of the plotting medium were prepared by adding 0.5 ml of the thrombin solution from Beriplast^{TM} P to 20 ml of a isotonic 0.03 mol/l calcium chloride solution (33.4 mg calcium chloride and 61.2 g sodium chloride). The process have been performed under sterile conditions to enable the use of scaffolds in cell culture. The machine was placed under a laminar flow hood and all the relevant parts were thermal sterilised. The fibrin glue was obtained in sterile packing and alginic acid was sterilised by using a gas-plasma. The plotting parameters were the following: $d_2 = 1.4$ mm, $d_3 = 0.45$ mm, $v = 18$ mm/s, $p = 1.2$–1.5×10^4 Pa, edge delay = 0.05 s.

The second 3D plotter, developed especially for the biofunctional processing was engineered by Envision Technologies (Marl, Germany). In contrast to the first machine, the software (PrimusData, Einsiedeln, Switzerland) was compatible to DXF-data and an import of volume data was possible. Furthermore, the hot temperature plotting head was electrical heated and a sensor controlled the position of the nozzle before starting the plotting process.

Alginic acid, 4-(2-Hydroxyethyl)-piperazin-1-ethansulfonic acid (used as buffer), phenol red (as dye) and hyaluronic acid have been obtained from Fluka. Standard agar from Difco (Detroit, USA) was used for the experiments. Human fibrinogen and thrombin (Beriplast^{TM} P) was obtained from Aventis Behring (Marburg, Germany). Gelatin was supplied by DGF Stoess (Eberbach, Germany) being a basic processed bone gelatin for pharmaceutical applications.

An environmental scanning electron microscope (ESEM 2020 from Electroscan Corp., Wilmington, USA) was used to examine the structure of hydrogels as well as the cells attached to the surface. The samples were cooled to 4.5°C and analysed under a water vapour of 867 Pa. This conditions prevented the samples mostly from drying. But for imaging reasons it was necessary to evaporate the water film on the top of the surface of the sample by lowering the water vapour pressure to around 500 Pa for two minutes. This short evaporation dehydrated the outer layers of the sample and caused a little crumbling of the cell structures as well as the hydrogel surface.

Mouse connective tissue fibroblasts were seeded on the hydrogel scaffolds. They were obtained from DSMZ (Braunschweig, Germany). The cell cultures on the scaffolds were performed in 96 well microplates and the different hydrogel scaffolds were placed into the microplates with 100 μl cell-medium. Then 100 μl cell-medium with 1×10^4 cells were brought into each well. The medium for the fibroblasts consisted of RPMI 1640 (Gibco Life Technologies, Inc., Grand Island, NY, USA) with 5% fetal calf serum (FCS, PAA), 2% HEPES (Gibco Life) and the antibiotics penicillin (100000 U/l) and streptomycin (100 mg/l) (both from Seromed, Berlin, Germany). The culture time in humidified atmosphere of 5% CO_2 at 37°C of an incubation machine (Hereus, Hanau, Germany) was 48 hours. After this time the cells were directly used for the proliferation test (EZ4Y) or conserved for SEM analysis by using an aqueous 8% formaldehyde solution.

3. Results

During the year 2000 a new 3D plotting process, that is based on a dispensing technique, was developed at the Freiburg Materials Research Center [10]. The difference of the 3D plotter to other dispensing techniques is the placement of the dispensing process into a bath of a liquid with matched density. The resulting gravity force compensation allows the dispensing of low viscosity plotting materials and widens the plotting material spectra. Therefore a very large variety of materials can be processed including melts, pastes, reactive resins or hydrogels. The basic principle of the 3D plotter is illustrated in Fig. 2.

It consists of a dispenser (with a optional heating jacket), that is movable in three dimensions. The plotting material, being stored in a cartridge, is plotted through a nozzle by air-pressure control into the liquid plotting medium. The densities and polarities of the liquid medium are carefully matched, thus preventing gravity-induced structural collapse. This very simple principle mostly eliminated the need for temporary support structures. It was possible to process a variety

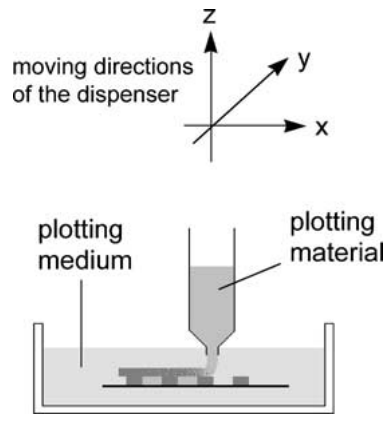

Figure 2 Basic principle of 3D plotting.

of the low viscous hydrogel precursors by applying a rapid prototyping technique.

The easiest case are thermoreversible hydrogels, like agar, which undergo a gelation if cooled below the gelling point. It was shown that the fabrication of agar scaffolds with a sufficient stability by using 3D plotting is possible [8]. A cubic agar scaffold with a length of 1 cm is displayed in Fig. 3.

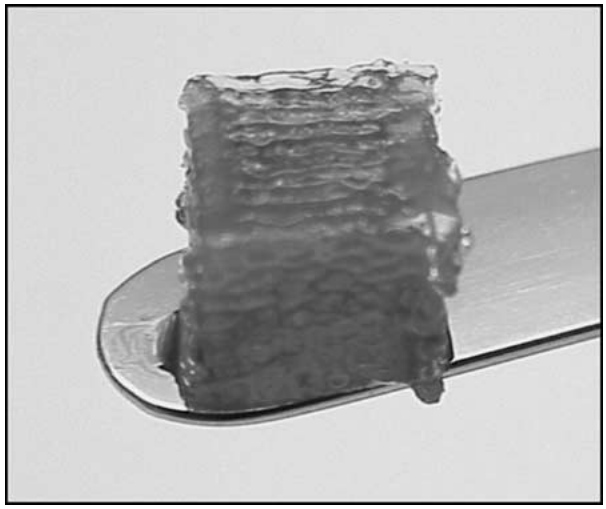

Figure 3 Agar scaffold prepared by 3D plotting (length 1 cm).

The heated plotting material was dispensed into a solution with a temperature below the gelation point of the hydrogel. The temperature of the plotting material was around 60°C–80°C depending on the concentration. It was also possible to seed and cultivate cells on the surface of these agar scaffolds. The scaffold surface was coated with hyaluronic acid to improve cell attachment. Fig. 4 shows a ESEM micrograph of a coated agar hydrogel strand entirely covered by fibroblasts after 2 days of cell culture.

Despite the successful processing of hydrogels demonstrated in this example the 3D plotting of agar does not fit all the requirements for a biofunctional processing. The problem is the elevated temperature that occurs in this process, which prevents the incorporation of proteins as well as living cells. To overcome this drawback another method of hydrogel processing was developed. In reactive plotting the plotting material contains a reactive component A which reacts with a reactive component B being dissolved in the plotting medium. It is essential that diffusion of component B from the plotting

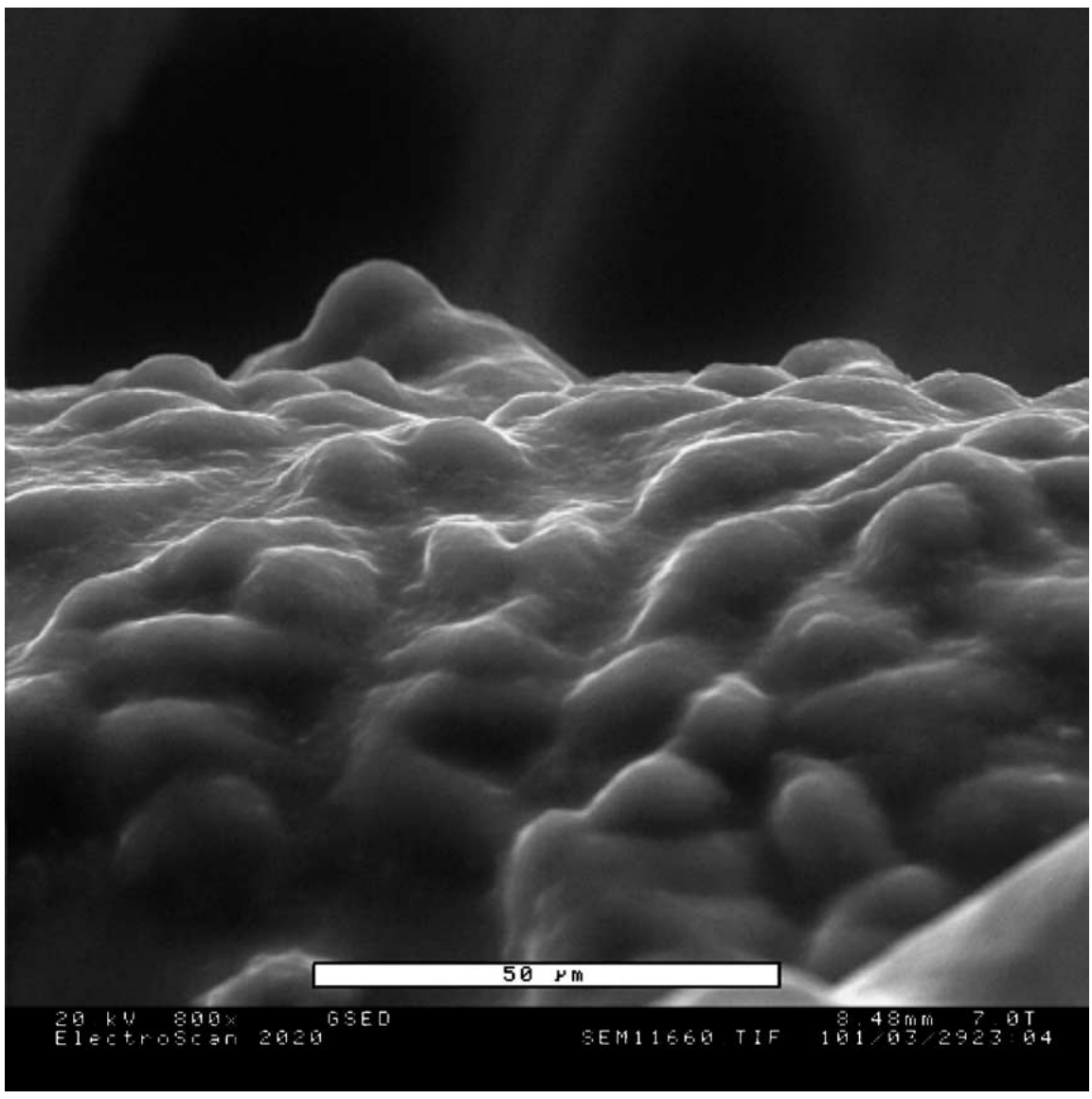

Figure 4 ESEM micrograph of mouse fibroblasts on the surface of a strand of an agar scaffold.

medium into the plotting material is much faster than the diffusion of component A into the surrounding plotting medium. Otherwise the chemical reaction between A and B would not take place in the plotting material but also in the surrounding plotting medium. But in general, the plotting material is desired to be solidified and therefore the component with the higher diffusion coefficient has to be placed in the plotting medium. From this point of view the reaction between a high molecular weight polymer with a very small diffusion coefficient and a low-molecular reactant is ideal for the reactive 3D plotting process. The complexation of polyelectrolytes by multivalent ions is a favourable reaction, because the reaction is fast, reliable, performed by using a cell and protein friendly chemistry and a wide array of non-toxic polyelectrolytes exist.

A solution of alginic acid was plotted into a calcium chloride solution. Alginic acid is a polysaccharide with carboxyl groups, that undergoes a fast complex formation with multivalent cations. After leaving the nozzle, the reaction occured, and the alginic acid solution became solidified. Due to the very fast reaction between the two components, the binding (interdiffusion of the polymer chains) between already solidified material and just dispensed material was insufficient. Therefore, it was necessary to reduce the speed of the reaction by adding a retarding agent. Suitable retarding agents are substrates with a higher complex binding constant to calcium than alginic acid. In this case the first calcium ions reaching the plotting material are trapped by the masking agent. The retarder becomes deactivated and the alginic acid solution remains sticky for some parts of a second. Examples of retarding agents are ethylenediamine tetraacetic acid (EDTA) or heparin. Only very small amounts of retarding agents are necessary but without it complete delamination was observed.

It is important to notice that the components are cell compatible and that the processing conditions do not restrict the usage of sensitive bioactive components. Unfortunately, the stability of scaffolds made out of calcium alginate is limited due to the fact that cell culture medium contains phosphate buffer. The phosphate precipitates the calcium, which crosslinks the alginic acid. A disintegration of the scaffold structure after some days in cell culture was the result. Choosing an other buffer system may solve the instability during cell culture but after implantation similar problems would rise up due to the insufficient chemical stability. Furthermore, alginic acid is not an ideal material for cell adhesion. Coating is suitable for surface growth of cells but not for the incorporation of cells into the material. A plotting material with an intrinsic good cell attachment is necessary. Therefore, a combination of alginic acid with fibrin was used. Because fibrin can be found in the human organism, it seems to be a perfect biomaterial and is well accepted by human cells. It is formed by the enzymatic reaction of fibrinogen with thrombin in the presence of calcium ions within 5–15 minutes. Due to this long solidification time, fibrin could not be processed alone. The solution of this problem was a two step solidification reaction. The plotting material contained a mixture of alginic acid and fibrinogen. The plotting medium was an aqueous solution of calcium chloride and thrombin. This solution was made isotonic by adding further salts (sodium chloride). In a first solidification step, alginic acid reacted in a fast complex formation with calcium ions turning the plotting medium into a stable gel. In a second step, the fibrinogen reacted with the thrombin in the plotting medium to form the fibrin. Again the diffusion coefficient of the thrombin was higher than from the fibrinogen. A scaffold obtained by reactive 3D plotting of alginic acid with fibrin is displayed in Fig. 5.

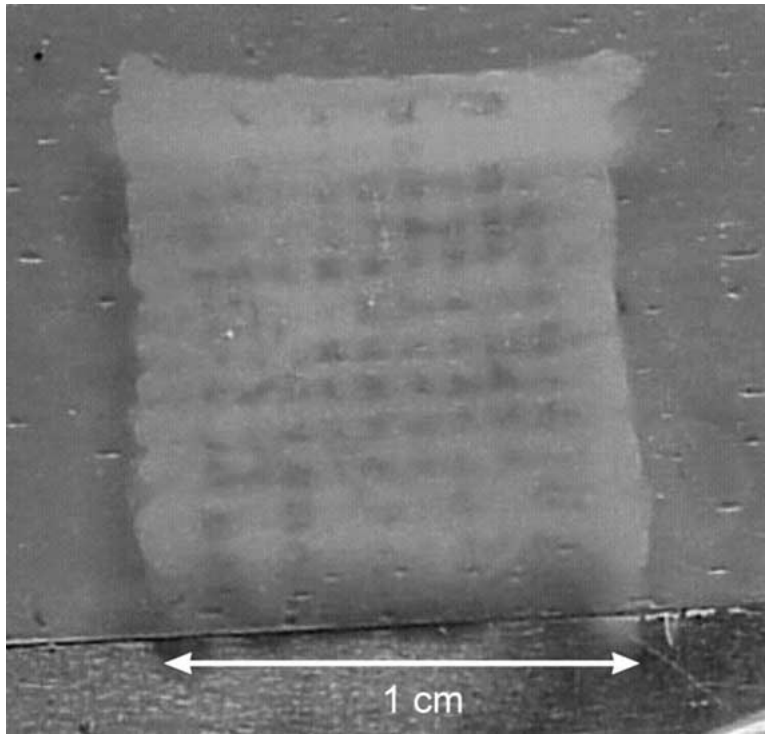

Figure 5 Scaffold from fibrin and alginic acid.

The scaffold in Fig. 5 contained around 20–25% of fibrin and 75–80% alginic acid in the dry mass (5% of the hydrogel). An increase of the fibrin content in future is possible, but it is necessary to maintain the viscosity of the plotting material at the same level. This is possible by adding gelatin or other polymers. The material combination of fibrin with alginic acid is important, because the process is cell friendly and the materials are biocompatible. Therefore, the incorporation of living cells into the alginic acid/fibrin hydrogel should be possible and therefore opens a broad range of potential applications in tissue engineering.

After finding a suitable material combination for the biomedical 3D plotting process, the characterisation of the scaffold structure is necessary for control of mechanical properties as well as cell growth. Especially the pore structure is a very important parameter of the scaffold structure because it determines permeability, mechanical properties and cell growth. The pore size was easily analysed by using light microscopy and was in the range of 200–400 μm for the hydrogel scaffolds. The porosity itself could be obtained from a comparison of the weight of the scaffold compared to a hydrogel cube of the same size. The values for the hydrogel

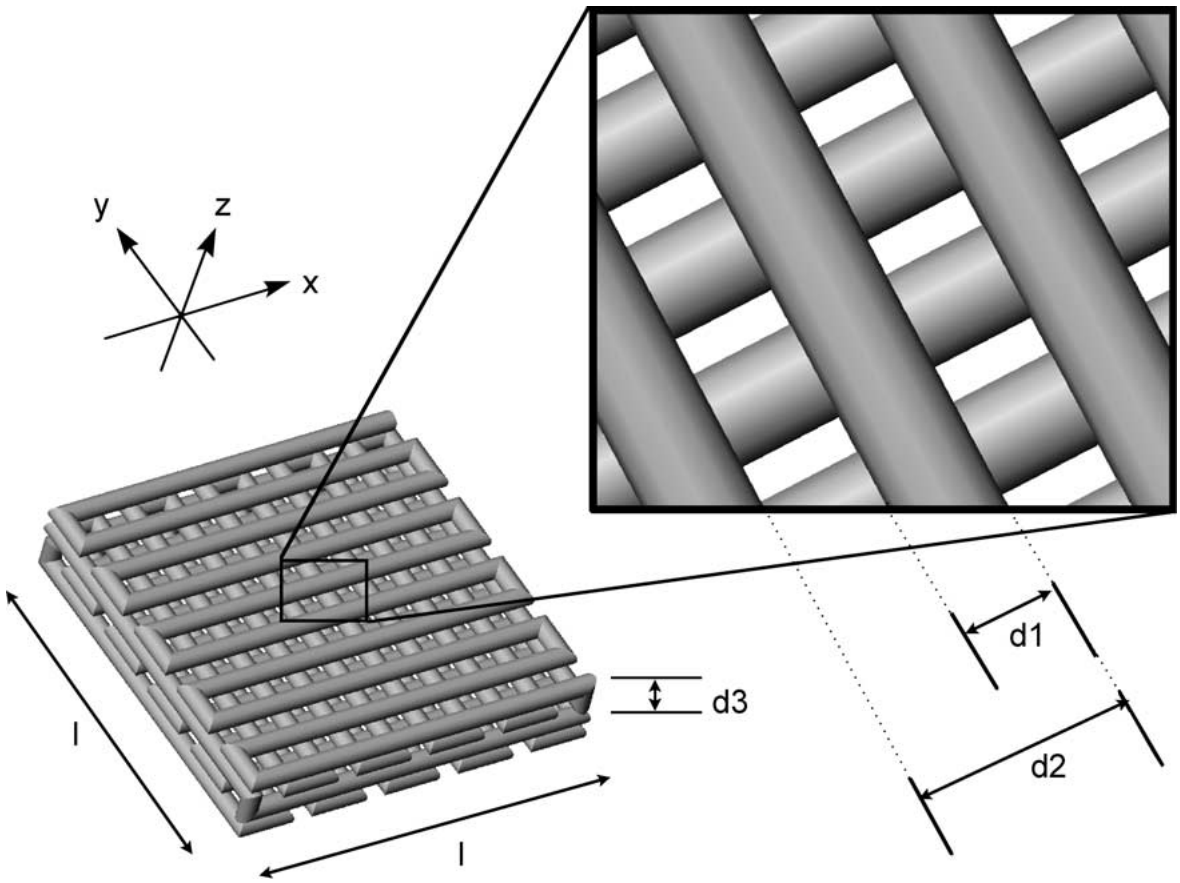

Figure 6 Simulated structure of a scaffold—definition of the plotting parameters.

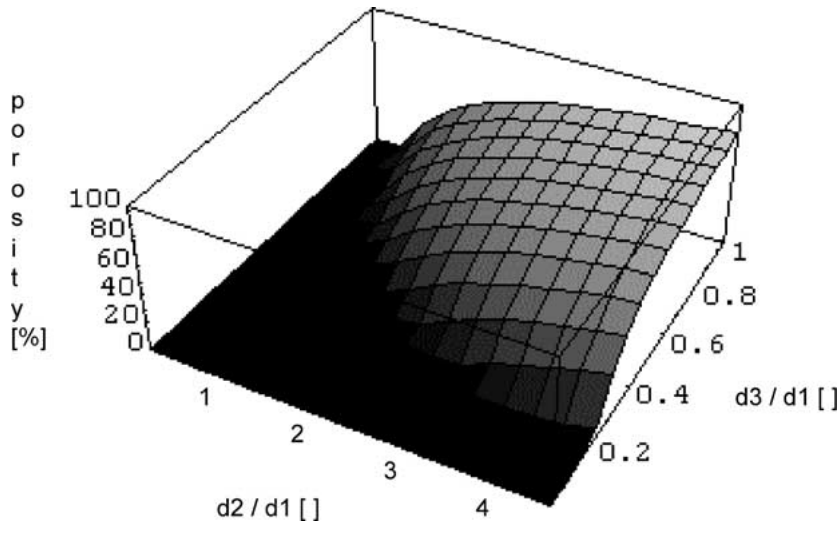

Figure 7 Dependence of the porosity from the reduced repeat lengths, see text.

scaffolds ranged from 40–55% depending on fabrication conditions. This experimental value can be compared to the theoretical values obtained from a cube of layers composed out of strands, in which every layer is turned around 90° against the neighbouring layers. A picture of a structure manufactured by 3D plotting is shown in Fig. 6.

For the following easy calculation the model of a cube of simple strands of circular cross section without contact points in the layer is used. The length is l, the strand diameter is d_1, the repeat length in the layer is d_2 and the repeat length in the vertical dimension (z) is d_3 as indicated by Fig. 6. The porosity depends on the scaffold volume (V_{scaffold}) and the volume of the full cube (V_{cube}). The scaffold volume is calculated by multiplying the volume of each layer (V_{layer}) with the number (n_z) of the repeat units (layers) in a vertical direction. The layer volume is easily obtained from the volume of each strand multiplied with the number of repeat units (strands) in the horizontal direction (xy).

$$l = n_{xy} \cdot d_2 = n_z \cdot d_3 \tag{1}$$

$$V_{\text{layer}} = n_{xy} \cdot \left(\frac{\pi}{4} \cdot d_1^2\right) \cdot l = \frac{l^2 \cdot \pi \cdot d_1^2}{4 \cdot d_2} \tag{2}$$

$$V_{\text{scaffold}} = n_z \cdot V_{\text{layer}} = \frac{\pi}{4} \cdot \frac{l^3 \cdot d_1^2}{d_2 \cdot d_3} \tag{3}$$

$$V_{\text{cube}} = l^3 \tag{4}$$

$$P = 1 - \frac{V_{\text{scaffold}}}{V_{\text{cube}}} = 1 - \frac{\pi}{4} \cdot \frac{1}{\left(\frac{d_2}{d_1}\right)} \cdot \frac{1}{\left(\frac{d_3}{d_1}\right)} \tag{5}$$

$$\text{Porosity}\,(\%) = \begin{cases} P \geq 0 & \text{Porosity} = \left(1 - \frac{\pi}{4} \cdot \frac{1}{\left(\frac{d_2}{d_1}\right)} \cdot \frac{1}{\left(\frac{d_3}{d_1}\right)}\right) \cdot 100 \\ P < 0 & \text{Porosity} = 0 \end{cases}$$

$$d_1, d_2, d_3 > 0; \quad \frac{d_2}{d_1} \in [0, \infty]; \quad \frac{d_3}{d_1} \in [0, 1] \tag{6}$$

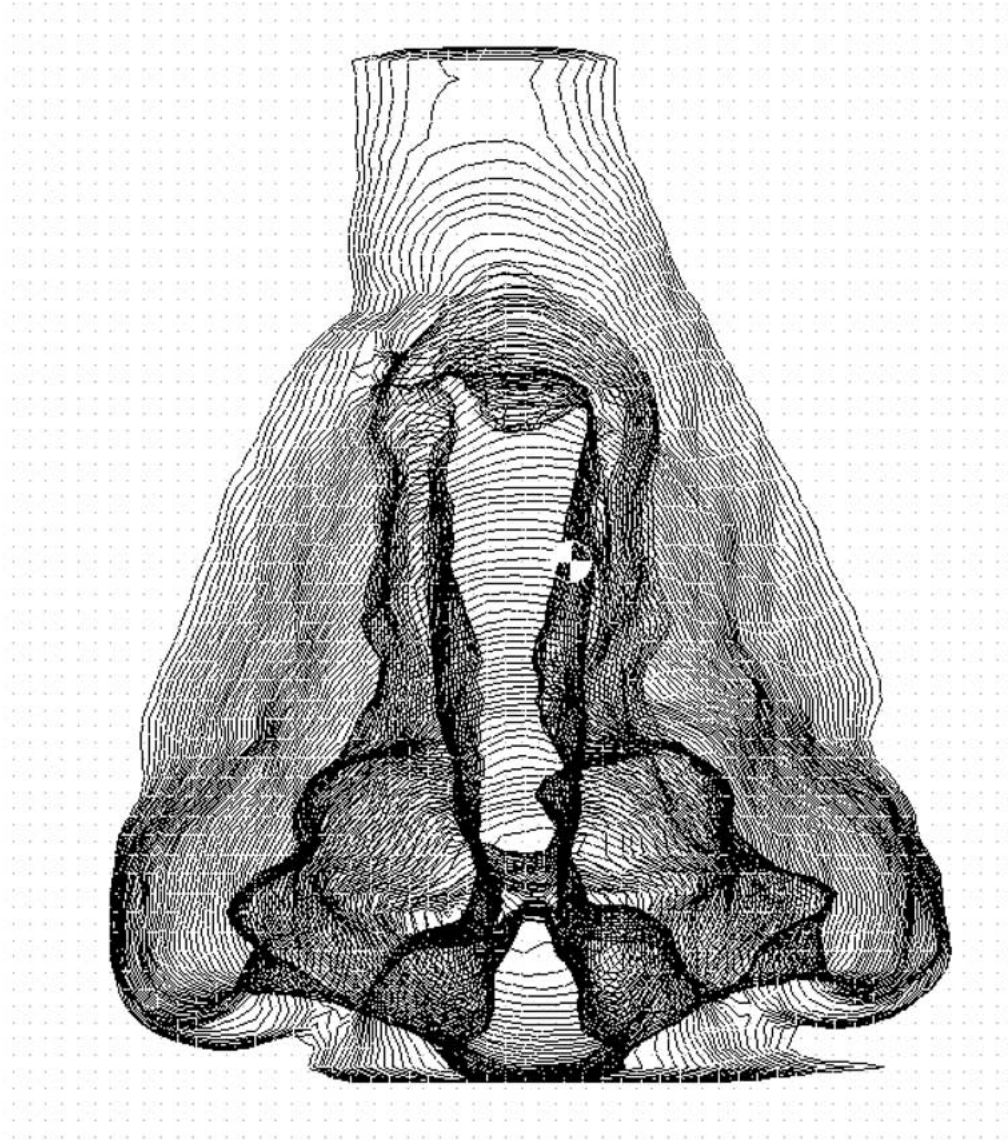

Figure 8 Computer model of a human nose. The model is sliced into subsequent layers of 300 μm thickness.

By using Equation 1, Equations 2 and 3 are easily derived. The parameter P in Equation 5 is obtained by comparison of scaffold volume to cube volume. The value of the scaffold porosity ranges from 0% up to 100%. Therefore, the negative values of the function P have to be substituted by 0 and Equation 6 is obtained defining the porosity of this simple model.

The porosity depends on two parameters: the ratios between the repeat length in xy-direction and in z-direction to the strand diameter. The dependence of the scaffold porosity on these two reduced repeat lengths is shown in Fig. 7.

The reduced repeat length in the xy-direction ranges from 0 up two high values. Typical values for the plotting process are 2 (gap diameter corresponds to the strand diameter) or 3 (gap diameter is twice the strand diameter). Higher values than 3 reduce the stability of the plotting process and are very difficult to realise. The reduced repeat length in z-direction is limited to values between 0 and 1. Values over 1 make no sense because delamination would result from a lost contact between the layers. Typical values in 3D plotting are 0.9 or 0.80 because a sufficient contact area between the layers is required to stick them together. The material of the overlapping area is deposited lateral to the contact area. Maximum porosity values of 50 up to 65% are derived from the reduced repeat length values given above. Higher porosities are nearly impossible from the practical point of view. The experimentally measured porosities were a little bit lower. The first reason is the approximation used for the simple porosity calculation (a cube of isolated strands has been used—not a structure build up by one single strand). Secondly difficulties during the experimental porosity measurement (remaining water in small pores) reduced the obtained porosity values. Finally practical deviations from the ideal structure due to effects like swelling or air pressure fluctuations which result in strand diameter variations distort the correspondence to the theoretical values.

In general RP technologies are able to produce any shape required. In contrast to this the structures of the scaffolds displayed in Figs 3 and 5 are very regular. This is due to the standard NC software of the first 3D plotter which required exact programming of the dispenser track in a Pascal like software syntax. The import of data from medical 3D analysis was impossible. Therefore, a new machine with improved software was designed to overcome this limitations. The first task of the software was to convert the volume data of the 3D model into layers. Fig. 8 displays the layers of a human nose including the cavities of the two nostrils. The layers have an equal distance of 300 μm, but smaller values up to 50 μm are possible.

Secondly the plotting path of each layer has to be created. Fig. 9a and b display two subsequent layers. The direction of the strands is turned rectangular. The enlargement of the left nostril (Fig. 9c) shows that the turning angle (between lengthened old moving direction and new moving direction) at the border of the 3D object has different values to fit the shape of the model in the best way. Turning angles below 45° and over 135° caused problems due to distortion during 3D plotting. Therefore, the software stopped the dispensing process every time the dispensing path reached such a point. Furthermore, an angle dependent delay was used for the turning points and for every start and stop of the plotting process due to the inertia of the plotting medium. These delays and the velocity of the process as well as the air pressure and nozzle type strongly depend on the material characteristics of the plotting material. Using this knowledge it was also possible to produce complex structures as indicated by Fig. 10.

Therefore, the "information path" of Fig. 1 starting from the 3D analysis methods and leading to the RP system is now considered to be mostly solved for 3D plotting.

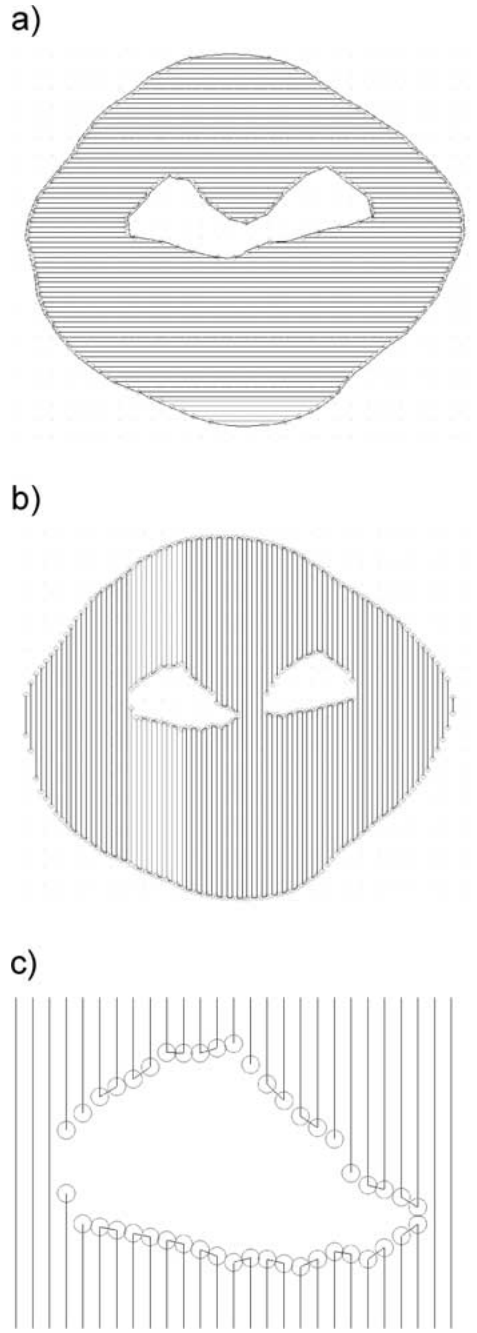

Figure 9 Generation of the plotting path in the layer: (a), (b) two subsequent layers of the nose and (c) enlargement of the left nostril in (b).

Figure 10 Silicone model of the nose prepared by 3D plotting.

4. Summary and discussion

The 3D plotting technology, combining RP technologies with tissue engineering, offers attractive opportunities for designing and desktop manufacturing of biomedical scaffolds and several applications in tissue engineering. Biocompatible rapid prototyping of hydrogels is introduced to fit the demands of tissue engineering. The reaction between plotting material and plotting medium was explored as reactive plotting to avoid high temperatures during scaffold fabrication. The reactive plotting is controlled by the chemical reaction itself and the diffusion coefficient of both reactants. In-situ-coating and formation of rough surface structures as well as fabrication of micro-tubes should be possible by adjusting the diffusion of the reactants. The two-step solidification of alginic acid and fibrin is cell compatible. This is an important step towards a biofunctional processing of soft tissue implants because this aqueous system has the potential to host bioactive components including cells, growth factors and drugs. The porosity of the resulting scaffolds were analysed and calculated for better understanding of the opportunities and limitations of the process. The free form fabrication of a nose by using a CAD model illustrates the layered manufacturing process and demonstrates the potential for soft tissue implant generation in future. Important challenges for further research are the incorporation of growth factors as well as living cells into the 3D plotting materials. Improvements regarding the mechanical properties and the growth of cells are necessary.

Acknowledgements

The authors thank the "Stifterverband für die Deutsche Wissenschaft" and the "Fonds der Chemischen Industrie" for financial support of this work.

References

1. G. B. STARK, R. HORCH and E. TANCZOS, "Biological Matrices and Tissue Reconstruction" (Springer, Berlin, 1998).
2. T. WOHLERS, Wohlers Report 2000, Wohlers Associates, Inc. Fort Collins, Colorado, 2000.
3. E. SACHS, M. CIMA, P. WILLIAMS, D. BRANCAZIO and J. CORNIE, *Journal of Engineering for Industry* **144** (1992) 481.
4. R. A. GIORDANO, B. M. WU, S. W. BORLAND, L. G. CIMA, E. M. SACHS and M. J. CIMA, *J. Biomater. Sci. Polymer Edn.* **8**(1) (1996) 63.
5. D. W. HUTMACHER, T. SCHANTZ, I. ZEIN *et al.*, *J. Biomed Mater. Res.* **55**(2) (2001) 203.
6. D. W. HUTMACHER, *Biomaterials* **21**(24) (2000) 2529.
7. K. Y. LEE and D. J. MOONEY, *Chemical Reviews* **101**(7) (2001) 1869.
8. W. M. KÜHTREIBER, R. P. LANZA and W. L. CHICK, "Cell Encapsulation Technology and Therapeutics" (Birkhäuser, Boston, 1998).
9. R. LANDERS, U. HÜBNER, R. SCHMELZEISEN and R. MÜLHAUPT, *Biomaterials*, submitted.
10. R. LANDERS and R. MÜLHAUPT, *Macromol. Mater. Eng.* **282** (2000) 17.

Received 3 June
and accepted 15 December 2001